



MARMARA UNIVERSITY
FACULTY OF ENGINEERING



AERODYNAMIC ANALYSIS
OF A GENERIC HYBRID SYSTEM

METE GÜLTEKİN

GRADUATION PROJECT REPORT
Department of Mechanical Engineering

Supervisor
Prof. Dr. Emre ALPMAN

ISTANBUL, 2023



**MARMARA UNIVERSITY
FACULTY OF ENGINEERING**



Aerodynamic Analysis of a Generic Hybrid System

by

Mete Gürtekin

July 3, 2023, Istanbul

**SUBMITTED TO THE DEPARTMENT OF MECHANICAL ENGINEERING
IN PARTIAL FULFILLMENT OF THE REQUIREMENTS FOR THE DEGREE**

OF

BACHELOR OF SCIENCE

AT

MARMARA UNIVERSITY

The author(s) hereby grant(s) to Marmara University permission to reproduce and to distribute publicly paper and electronic copies of this document in whole or in part and declare that the prepared document does not in any way include copying of previous work on the subject or the use of ideas, concepts, words, or structures regarding the subject without appropriate acknowledgement of the source material.

Signature of Author(s) Mete GÜLTEKİN

A handwritten signature in black ink, appearing to read 'Mete Gürtekin'.

Department of Mechanical Engineering

Certified By Prof. Dr. Emre ALPMAN

Project Supervisor, Department of Mechanical Engineering

Accepted By Prof. Dr. Bülent EKİCİ

Head of the Department of Mechanical Engineering

ACKNOWLEDGEMENT

First of all, I would like to thank my supervisor Prof. Dr. Emre Alpman, for the valuable guidance and advice on preparing this thesis and giving me moral and material support.

I would also like to thank my family for their moral support during the preparation of this thesis and for making me feel that they are always with me.

July, 2023

Mete Gültekin

CONTENTS

ACKNOWLEDGEMENT.....	ii
CONTENTS	iii
ÖZET.....	4
ABSTRACT	5
SYMBOLS	6
ABBREVIATIONS	7
LIST OF FIGURES	8
LIST OF TABLES.....	9
1. INTRODUCTION.....	10
2. MATERIALS AND METHODS	12
3. RESULTS AND DISCUSSION.....	19
4. CONCLUSIONS	27
5. REFERENCES.....	28
6. APPENDICES.....	29

ÖZET

Genel bir Hibrit Sistemin Aerodinamik Analizi

Bu tez, dikey kalkış ve iniş ve verimli ileri uçuş yapabilen (VTOL) hibrit bir sistem olan “tailsitter” dronların aerodinamik analizini sunmaktadır. İlk olarak, belirli konfigürasyonlar ışığında bir tasarıma karar verilir. Tasarım daha sonra bir CAD programı kullanılarak bilgisayarda çizilir. Yapılan analiz ile uçağın Kaldırma Katsayısı (CL) ve Sürükleme Katsayısı (CD) değerleri bulunur. Bulunan Kaldırma Katsayısı (CL) deneysel sonuçlarla karşılaştırılır. Uçağı etkileyen basınç, sıcaklık ve diğer faktörler de analiz edilir.

Bulgular, “tailsitter” olarak uçuş gerçekleştirecek bir insansız hava aracı (İHA) tasarımının genel bir aerodinamik analizini sunmaktadır ve bu dronların aerodinamiğinin anlaşılması artırarak kontrol stratejilerinin ve operasyonel uygulamaların geliştirilmesine rehberlik etmektedir. Araştırma, gözetim, teslimat hizmetleri ve havadan denetimlerin ilerlemesine de katkıda bulunmaktadır.

ABSTRACT

Aerodynamic Analysis of a Generic Hybrid System

This thesis presents an aerodynamic analysis of "tailsitter" drones, a hybrid system capable of vertical take-off and landing (VTOL) and efficient forward flight. First, a design is decided upon in light of specific configurations. The design is then drawn on a computer using a Computer Aided Design (CAD) program. With the analysis, the Coefficient of Lift (C_L) and Coefficient of Drag (C_D) values of the aircraft are found. The Coefficient of Lift (C_L) is compared with experimental results. Pressure, temperature and other factors affecting the aircraft are also analyzed.

The findings provide a general aerodynamic analysis of an unmanned aerial vehicle (UAV) design to fly as a "tailsitter" and guide the development of control strategies and operational practices by increasing the understanding of the aerodynamics of these drones. The research also contributes to the advancement of surveillance, delivery services and aerial inspections.

SYMBOLS

A : Wing area (m^2)

C_L : Coefficient of lift

C_D : Coefficient of drag

D : Drag force (N)

L : Lift force (N)

ρ : Air density (kg/m^3)

V : Airspeed (m/s)

L_c : Characteristic length (m)

ν : Kinematic viscosity (m^2/s)

α : Angle of attack (degrees)

ABBREVIATIONS

UAV : Unmanned Aerial Vehicle

CFD : Computational Fluid Dynamics

CAD : Computer Aided Design

VTOL : Vertical Takeoff and Landing

FEA : Computational Fluid Dynamics

LIST OF FIGURES

	PAGE
Figure 1.1 One of the tailsitter designs: The Convair	10
Figure 1.2 Transition of Tailsitters	11
Figure 2.1 The Tailsitter Drone Design.....	13
Figure 2.2 Naming distances to calculate characteristic length (L_C).....	14
Figure 2.3 Wing parameters of drone.....	14
Figure 2.4 Enclosure.....	15
Figure 2.5 Desired goals.....	16
Figure 2.6 Right view of mesh.....	16
Figure 2.7 Zoomed out view of mesh from right view.....	17
Figure 2.8 Front view of mesh.....	17
Figure 2.9 Iteration process.....	18
Figure 3.1 Area of one wing.....	19
Figure 3.2 C_L - angle of attack (α) values of SD7003 airfoil.....	20
Figure 3.3 Right view of velocity(z) contours.....	22
Figure 3.4 Isometric view of velocity(z) trajectories.....	23
Figure 3.5 Top view of velocity(z) trajectories.....	23
Figure 3.6 Right view of velocity(z) trajectories.....	24
Figure 3.7 Right view of pressure contours.....	24
Figure 3.8 Isometric view of pressure contours.....	25
Figure 3.9 Right view of temperature contours.....	25
Figure 3.10 Front view of temperature contours.....	26

LIST OF TABLES

PAGE

Table 2.1 Hybrid UAV types.....	12
Table 3.1 Results of goals.....	21
Table 3.2 Max-min values of goals.....	22

1. INTRODUCTION

1.1. Background and Motivation

Unmanned aerial vehicles' (UAVs') rapid development has created new opportunities for a variety of uses, including surveillance, delivery services, and aerial inspections.

Tailsitter drones, a promising hybrid system that combines vertical takeoff and landing (VTOL) capabilities with effective forward flight, have emerged among the various UAV configurations. In the field of aerodynamics, tailsitter drones' distinctive design and ability to transition from vertical to horizontal flight pose both exciting opportunities and difficult challenges.



Figure 2.1 One of the tailsitter designs: The Convair Pogo

The ability of tailsitter drones to combine vertical takeoff and landing (VTOL) capabilities with effective forward flight is their main advantage. This enables them to operate in a variety of environments, such as congested areas, cities, and remote areas without access to traditional runways or landing strips. Due to their excellent maneuverability and quick transition between hovering and forward flight, tailsitters are well suited for a variety of tasks, including delivery, passenger transportation, surveillance, and reconnaissance.

Tailsitter drones typically combine fixed-wing and multirotor technologies to achieve vertical takeoff and landing. Similar to a conventional multicopter, the drone's rotors or propellers provide the lift required to ascend vertically during takeoff. The drone tilts its entire body or particular wing sections to enter a horizontal flight mode once it reaches the desired altitude. As with a fixed-wing aircraft, this transition enables the wings to produce lift in the forward flight configuration. Typically, onboard flight control systems automate and regulate the transition process.

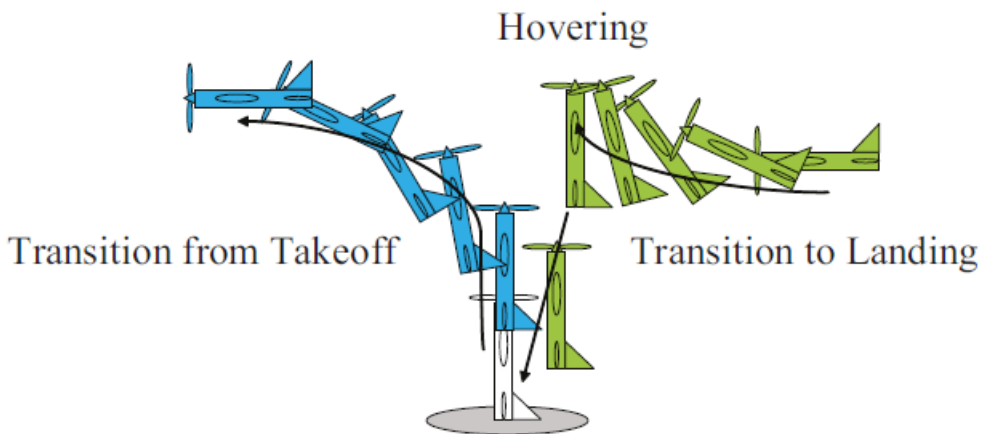


Figure 1.3 Transition of Tailsitters

Tailsitter drones' aerodynamics are essential to their effective and stable flight. Similar to a helicopter, the drone uses its rotors or propellers to create lift during vertical flight. To guarantee proper control and stability during vertical flight, the orientation and configuration of these lift-producing elements are essential. In horizontal flight, the elevators, ailerons, and rudders serve as the control surfaces and produce the majority of the lift.

Tailsitter drones' aerodynamic analysis involves looking at a variety of elements, such as the wing design, control surfaces, flight control algorithms, stability, efficiency, and performance traits. These drones' aerodynamic behavior can be studied using techniques like wind tunnel testing and computational fluid dynamics (CFD) simulations. To further optimize the overall performance of the tailsitter drone, factors like weight distribution, center of gravity, and power requirements must be taken into consideration.

1.2 Problem Statement

The performance, stability, and control of tailsitter drones must be maximized through aerodynamic analysis. The aerodynamic effects on tailsitter drones during horizontal flight should be found. The results should be explained with visual figures and the findings should be compared with experimental data.

1.3 Objectives

The purpose of this study is to conduct a comprehensive aerodynamic analysis of tailsitter drones. Aim is to design and analyze an efficient tailsitter drone and compare it with experimental data. The design will then be ready for operational use.

1.4 Approach

To achieve the objectives of this study, a combination of computer-aided design (CAD) software and computational fluid dynamics (CFD) simulations will be employed. The CAD software will be utilized to design a tailsitter drone model. The designed model will then be subjected to CFD simulations using PC software.

1.5 Structure of the Report

This report is organized into several chapters to provide a coherent and comprehensive understanding of the aerodynamic analysis of tailsitter drones. Chapter 2 presents the materials and methods, chapter 3 gives the results and discussion, chapter 4 focuses on the conclusion and chapter 5 presents the references. Finally, Chapter 6 is appendices.

Through this study, it is anticipated that a deeper understanding of the aerodynamics of tailsitter drones will be achieved, facilitating the development of more efficient and maneuverable hybrid systems for a wide range of applications.

2. MATERIALS AND METHODS

2.1 Tailsitter Drone Design

The first step in performing an aerodynamic analysis of tailsitter drones was to design a representative model. In this chapter, a VTOL design was decided upon based on some considerations. A 3D model of the tailsitter drone was created using computer-aided design (CAD) software.

The design process involved defining the overall dimensions, wing geometry, rotor configuration, and control surfaces. The wing aspect ratio, sweep angle, and airfoil selection were carefully chosen to ensure optimal lift and drag characteristics. The rotor arrangement, whether quadcopter or coaxial, was evaluated for its impact on lift generation, efficiency, and control authority during vertical and transitional flight phases. Control surfaces, such as elevons, were incorporated for maneuverability and control effectiveness.

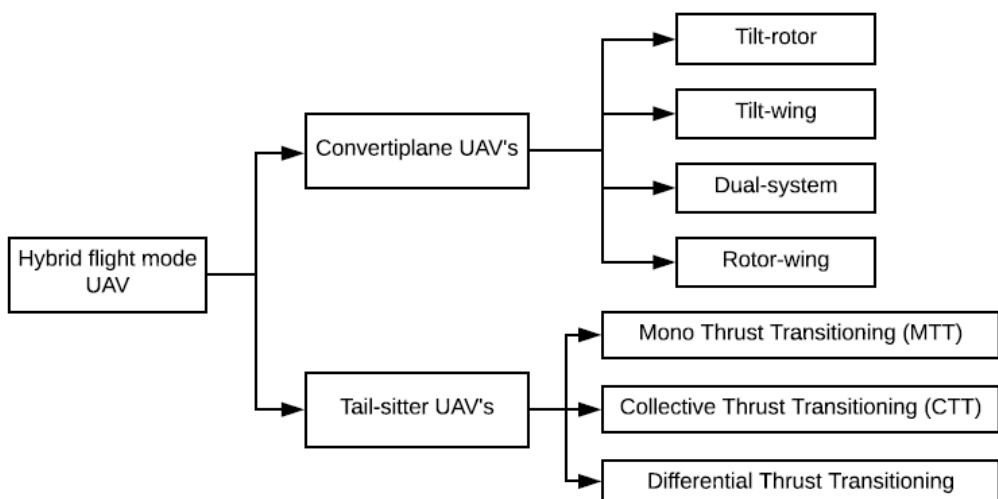


Table 2.1 Hybrid UAV types

It was then decided to design an aileronless (elevator only), front twin-engine aircraft with radiused tapered wings. This design was preferred as it would be more stable and powerful in vertical take-off. It will also provide optimum stability and balance in horizontal flight and transition. SD7003 was selected as the wing airfoil. The SD7003 is known for its good high-speed performance and marginal thermal performance.

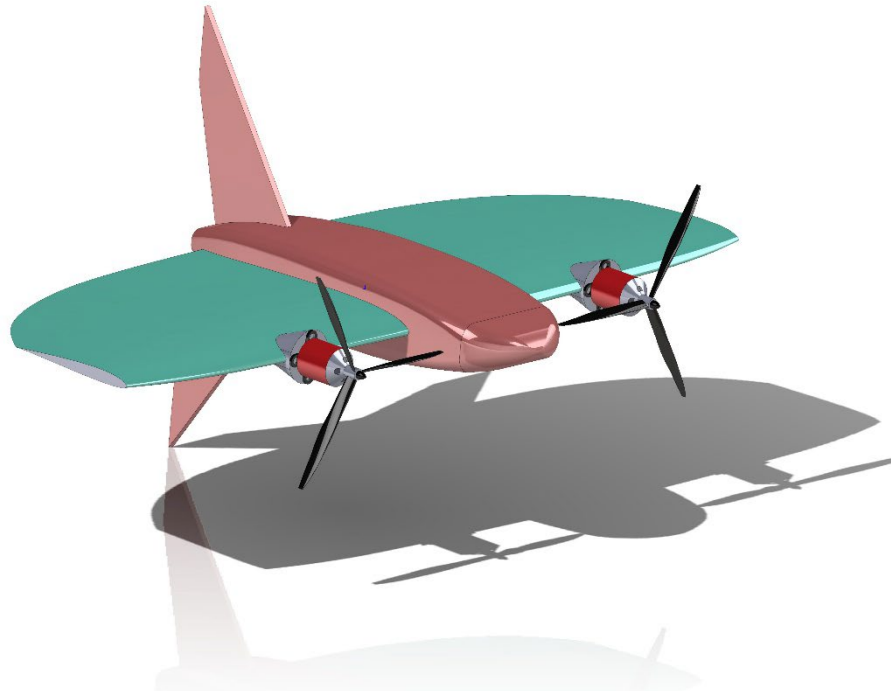


Figure 2.1 The Tailsitter Drone Design

2.2 Calculations, Computational Fluid Dynamics (CFD) Analysis and Simulations

To analyze the aerodynamic behavior of the designed tailsitter drone, computational fluid dynamics (CFD) simulations were conducted using PC software. The CFD simulations enabled a detailed examination of the airflow around the drone, providing valuable insights into the lift, drag, and stability characteristics.

The airplane will fly at low speeds. Since the data of 300000 Reynolds Number is available as experimental data, the airplane speed is adjusted accordingly. [1]

$$Re = \frac{\text{Inertial Forces}}{\text{Viscous Forces}} = \frac{VL_c}{\nu}$$

$$V = \frac{\nu * Re}{L_c}$$

$$Re = 300000$$

$$\nu = \text{kinematic viscosity of the air at } 20^\circ\text{C} = 1.516 * 10^{-5} \frac{\text{m}^2}{\text{s}}$$

[2]

To find mean characteristic length (L_c), we can use this formula:

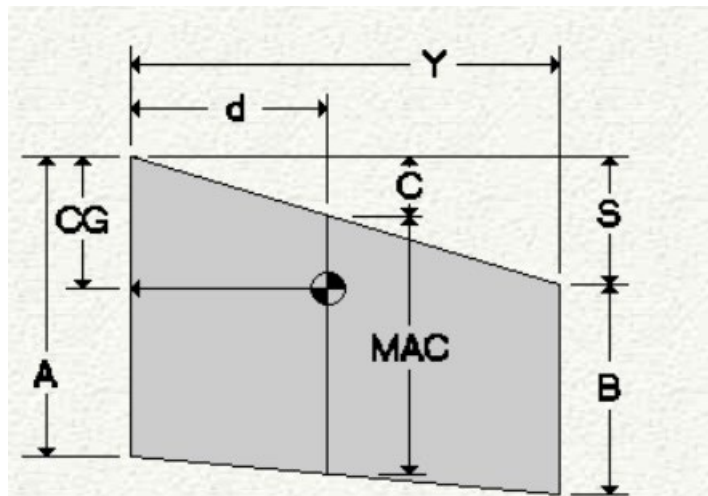


Figure 2.2 Naming distances to calculate characteristic length (L_c)

$$L_c = \text{Characteristic Length} = \text{MAC} = A - (2(A - B)(0.5A + B) / (3(A + B)))$$

[3]

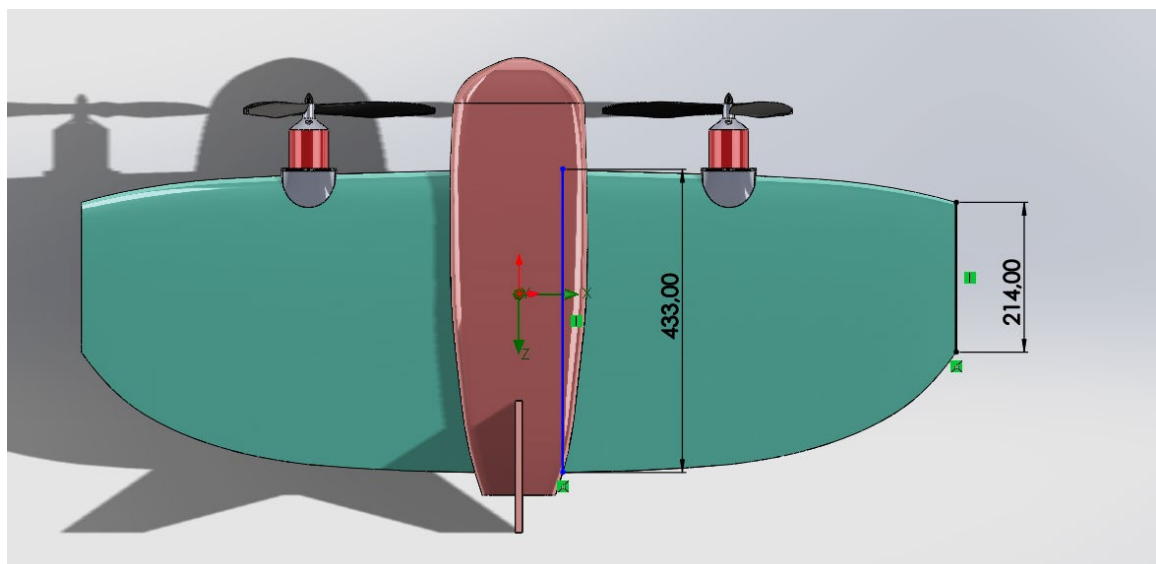


Figure 2.3 Wing parameters of drone

For our design:

$$A = 433 \text{ mm} = 0.433 \text{ m}$$

$$B = 214 \text{ mm} = 0.214 \text{ m}$$

Then;

$$L_c = 0.3359 \text{ m}$$

So,

$$V = \frac{\nu * Re}{L_c} = \frac{1.516 * 10^{-5} * 300000}{0.3359} = 13.54 \text{ m/s}$$

Therefore, our drone will fly at velocity of 13.54 m/s. In other words, the velocity of the air in the flow analysis in our CFD program will be 13.54 m/s.

We start the analysis by choosing our speed as 13.54 m/s, temperature as 20°C and pressure as 101325 Pa.

The SI unit system was used as the unit system and the gravitational force was adjusted in the direction of the y-axis, because the y-axis is the axis perpendicular to the plane in the program. Air was selected as the fluid. The program pulls the characteristic values of the gas from the embedded settings.

A suitable enclosure was created. 1 m up and down, 1 m left and right, 2.3 m in front and 3.6 m behind. In this way, the incoming fluid will be able to flow sufficiently and the calculation errors caused by its closeness to the body will be eliminated.

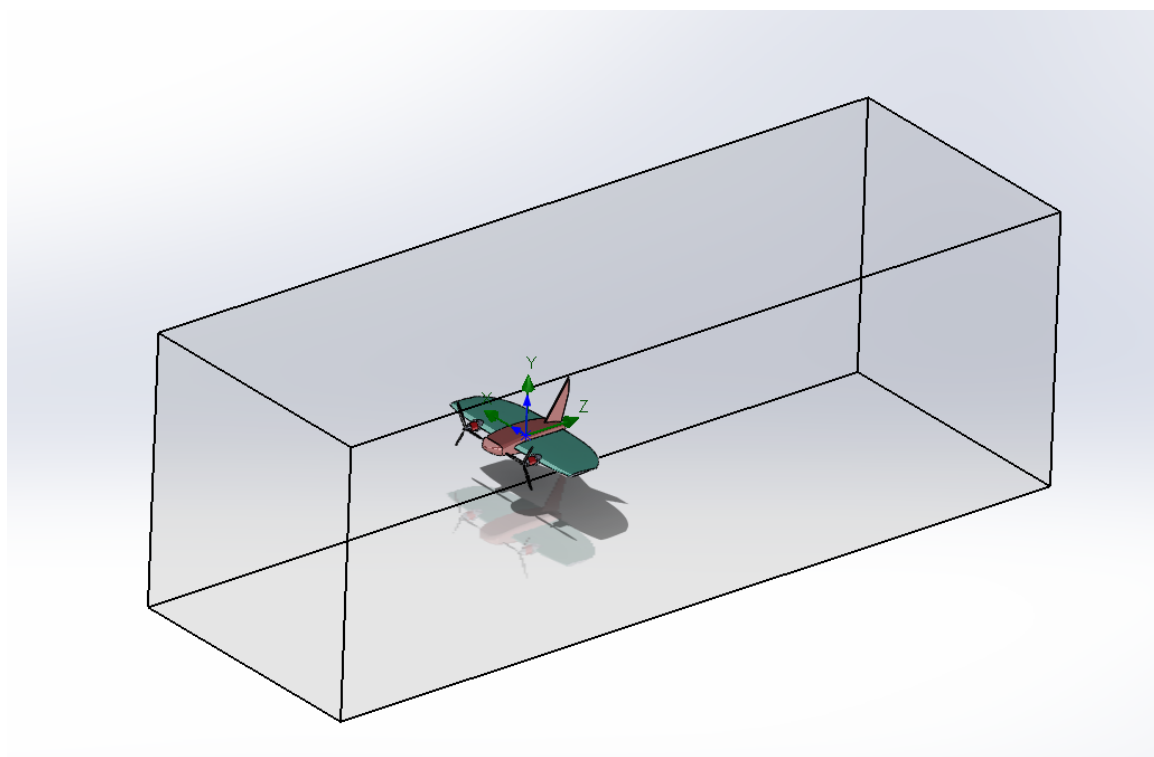


Figure 2.4 Enclosure

The desired goals were selected.



Figure 2.5 Desired goals

We proceeded to mesh settings and global mesh was made first. A fine mesh was tried to be set. Local meshing was also done to create a more precise mesh around the body. In this way, the analysis will be more efficient and will give accurate results. At the end of the mesh, 1450111 cells were created.

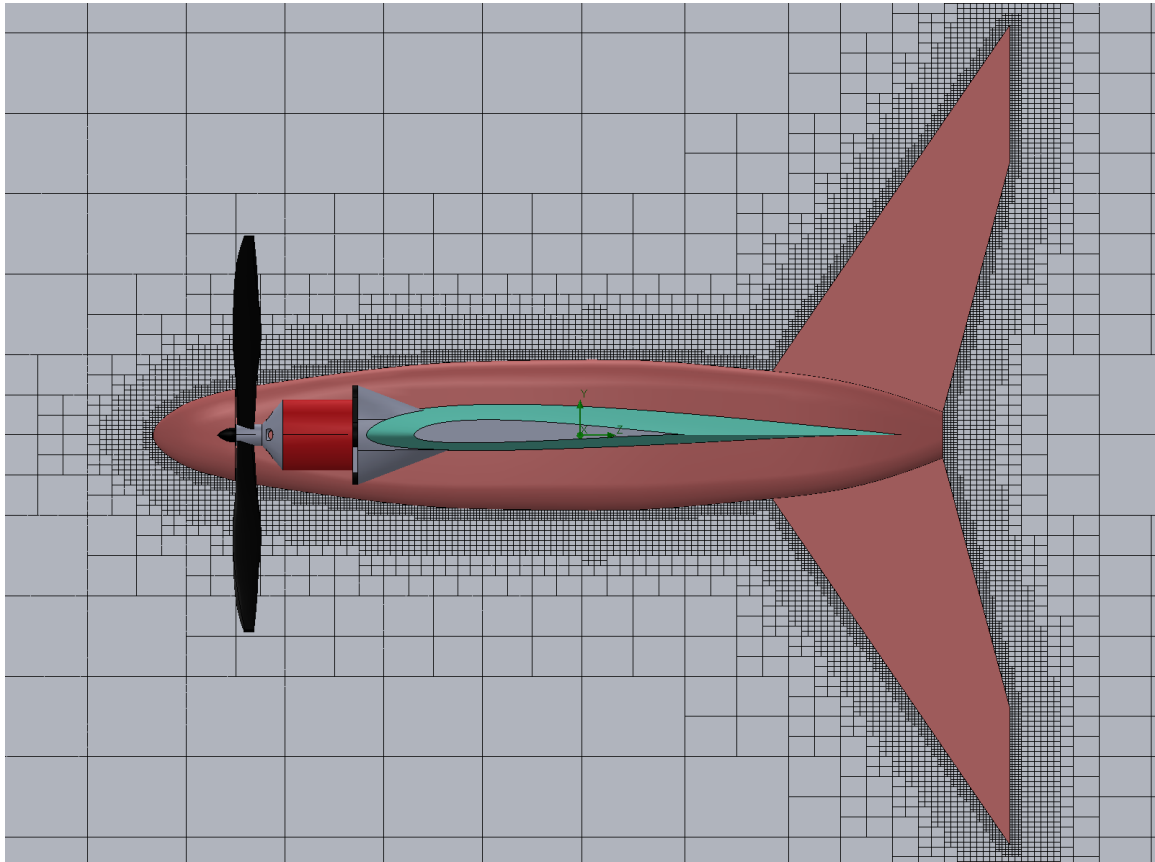


Figure 2.6 Right view of mesh

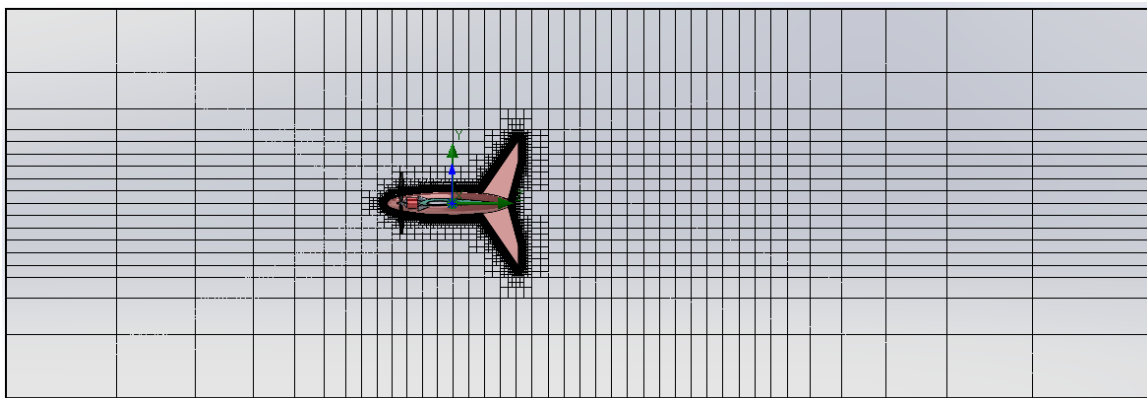


Figure 2.7 Zoomed out view of mesh from right view

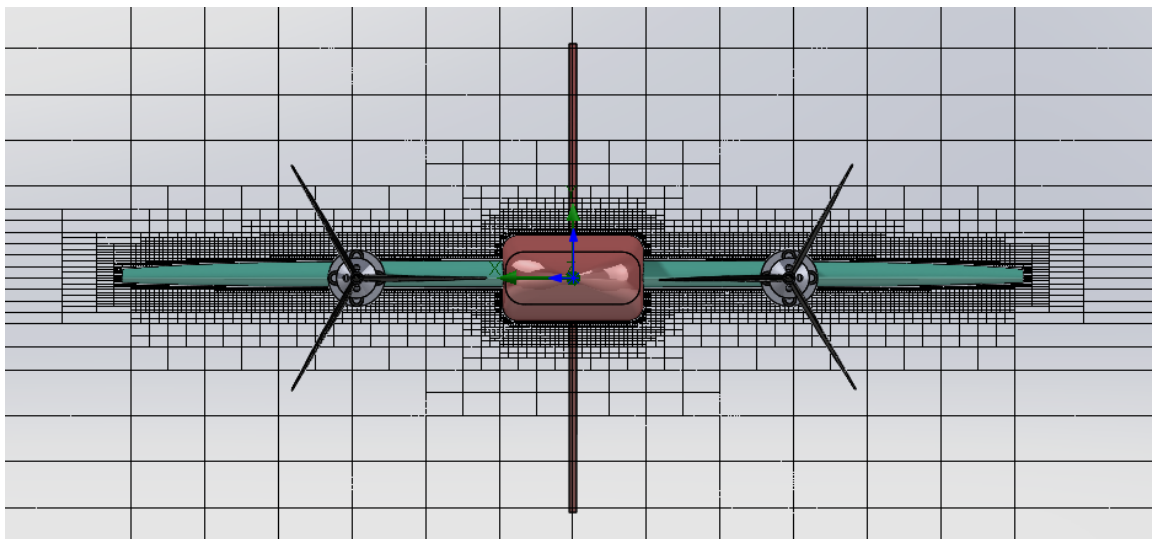


Figure 2.8 Front view of mesh

Then the calculation part started. After enough iterations (227th iteration) all values were found with the desired precision. The graph below shows a normalized scale plot of these values.

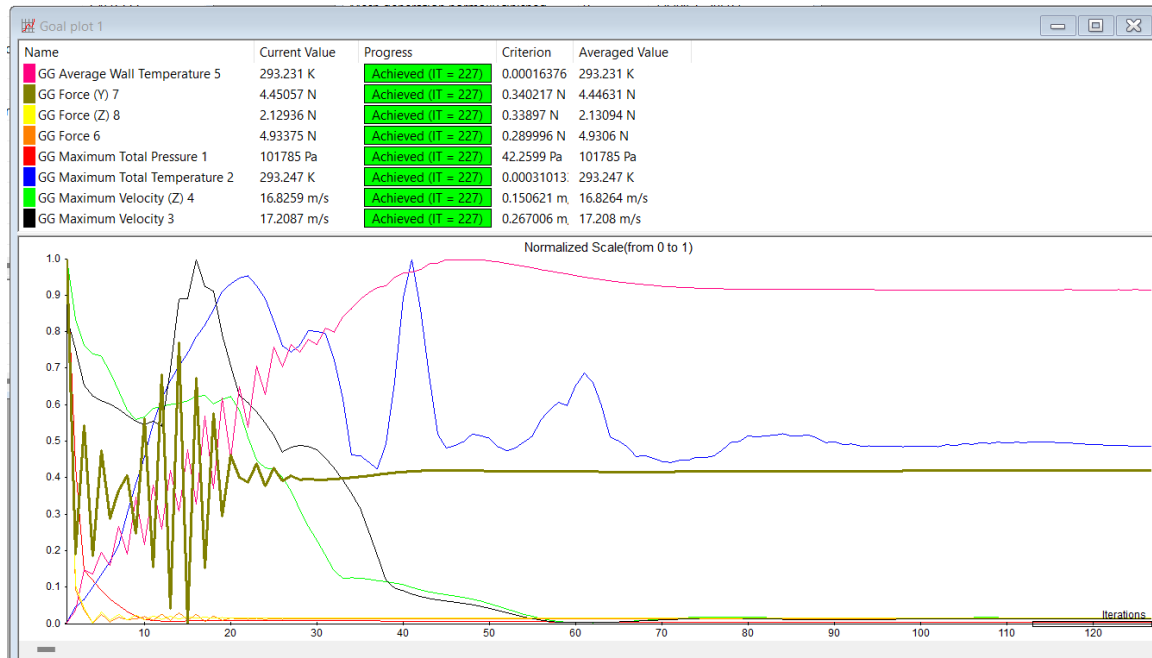


Figure 2.9 Iteration process

3. RESULTS AND DISCUSSION

In this chapter, the values found as a result of the analysis will be listed and the coefficient of lift (C_L) value will be compared with the experimental data.

$$C_L = \frac{L}{\frac{1}{2} \rho V^2 A}$$

$$C_D = \frac{D}{\frac{1}{2} \rho V^2 A}$$

As can be seen, as a result of the analysis, the lift (L) value was found to be 4.451 N and the drag (D) value was found to be 2.129 N. Now the "A" value, i.e. the reference wing area, must be found. For this, the area of the single wing was found in the drawing on the software and then multiplied by 2.

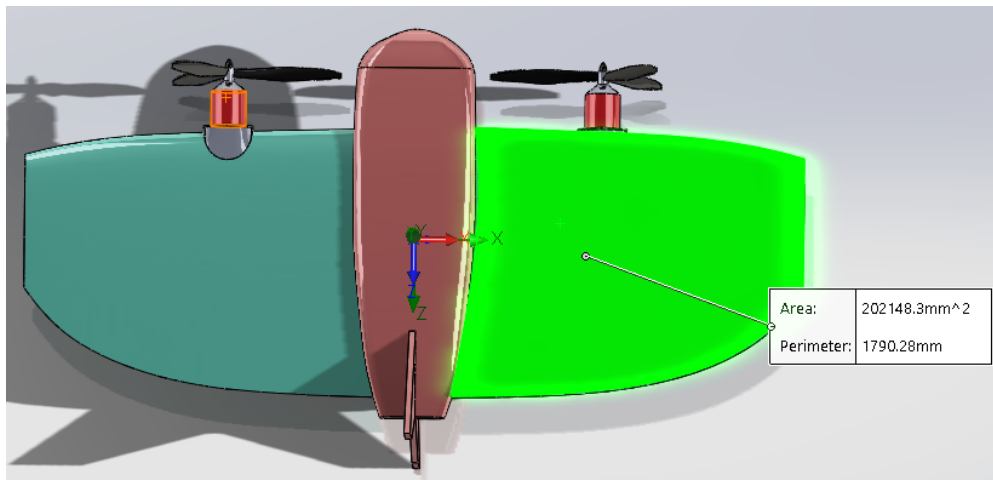


Figure 3.1 Area of one wing

$$A = \text{Reference Wing Area} = 2 * 202148.3 \text{ mm}^2 = 0.404296 \text{ m}^2$$

$$\begin{aligned} L &= 4.451 \text{ N} \\ D &= 2.129 \text{ N} \end{aligned}$$

$$\rho = \text{density of the air at } 20^\circ\text{C} = 1.2041 \frac{\text{kg}}{\text{m}^3}$$

[4]

$$V = 13.54 \text{ m/s}$$

Now, we will use these values to find C_L and C_D .

$$C_L = \frac{L}{\frac{1}{2} \rho V^2 A} = \frac{4.451}{\frac{1}{2} * 1.2041 * 13.54^2 * 0.404296} = 0.0997$$

$$C_D = \frac{D}{\frac{1}{2} \rho V^2 A} = \frac{2.129}{\frac{1}{2} * 1.2041 * 13.54^2 * 0.404296} = 0.0477$$

We will now compare this C_L value with the experimental findings on page 209 of volume 1 of Summary of Low-Speed Airfoil Data by "Michael S. Selig, James J. Guglielmo, Andy P. Broeren and Philippe Giguere". [4]

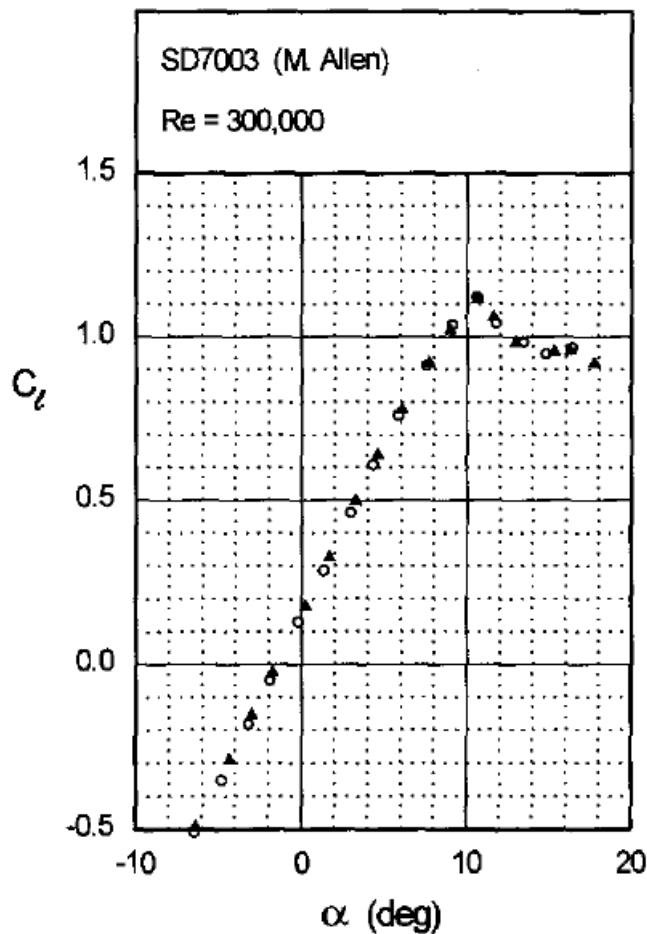


Figure 3.2 C_L - angle of attack (α) values of SD7003 airfoil [5]

In our analysis, the angle of attack (α) is taken as 0. This is because the airplane flies horizontally. Looking at the C_L value corresponding to 0 from the graph, a value of approximately 0.11 can be seen.

If we want to find the error rate and accuracy with the data we found:

$$Accuracy = 100 - 100 * \frac{(0.11 - 0.0997)}{0.11} = \%90.64$$

It is seen that a very sufficient accuracy rate was achieved. This is evidence that the analysis and simulation was efficient and appropriate.

Other findings of the analysis are as follows:

Name	Unit	Value	Criteria	Delta
GG Maximum Total Pressure 1	Pa	101784.5 1	42.2599467	2.02557366
GG Maximum Total Temperature 2	K	293.25	0.00031013 3205	0.0002164983 72
GG Maximum Velocity 3	m/s	17.209	0.26700647 5	0.0145025323
GG Maximum Velocity (Z) 4	m/s	16.826	0.15062120 3	0.0149596128
GG Average Wall Temperature 5	K	293.23	0.00016376 1159	2.33592665e-05
GG Force 6	N	4.934	0.28999580 4	0.0184189511
GG Force (Y) 7	N	4.451	0.34021688 1	0.0197259667
GG Force (Z) 8	N	2.129	0.33897019 4	0.0035762263 9

Table 3.1 Results of goals

Name	Minimum	Maximum
Density (Fluid) [kg/m^3]	1.20	1.21
Pressure [Pa]	101164.60	101797.96
Temperature [K]	293.09	293.24
Temperature (Fluid) [K]	293.09	293.24
Velocity [m/s]	0	17.224
Velocity (X) [m/s]	-11.196	11.891
Velocity (Y) [m/s]	-12.219	12.235
Velocity (Z) [m/s]	-7.038	16.840
Normal []	1.0000000	1.0000000
Mach Number []	0	0.05
Velocity RRF [m/s]	0	17.224
Velocity RRF (X) [m/s]	-11.196	11.891
Velocity RRF (Y) [m/s]	-12.219	12.235
Velocity RRF (Z) [m/s]	-7.038	16.840

Vorticity [1/s]	4.60e-04	8189.77
Distributed Force [Pa]	101177.81	101791.84
Relative Pressure [Pa]	-160.40	472.96
Shear Stress [Pa]	0	46.16
Bottleneck Number []	1.0421215e-12	1.0000000
Heat Transfer Coefficient [W/m^2/K]	0	0
ShortCut Number []	2.2176309e-13	1.0000000
Surface Heat Flux [W/m^2]	0	0
Surface Heat Flux (Convective) [W/m^2]	0	0
Total Enthalpy Flux [W/m^2]	-4860045.19	4859052.244
Acoustic Power [W/m^3]	0	8.295e-07
Acoustic Power Level [dB]	0	59.19

Table 3.2 Max-min values of goals

Visual simulations & findings:

As can be seen from the speed simulations below, the speed decreases at the nose of the airplane and at the rear of the tail. It is also clear that turbulence occurs at the rear of the engines and at the very rear and center of the tail.

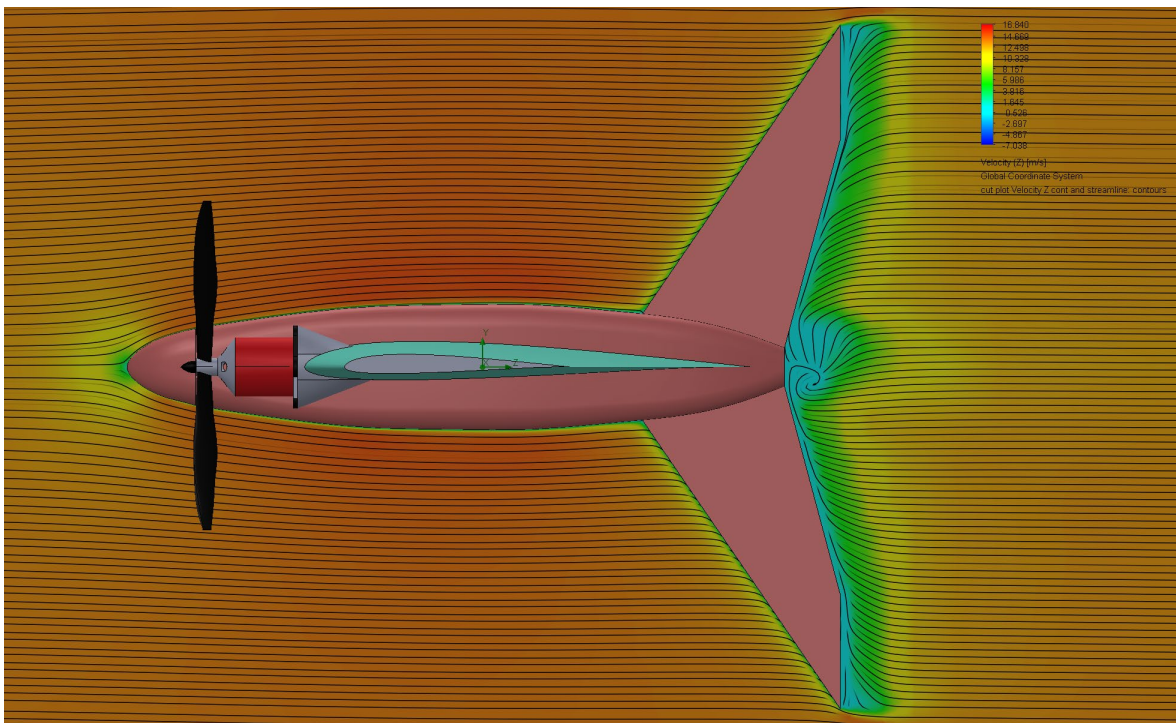


Figure 3.3 Right view of velocity (z) contours

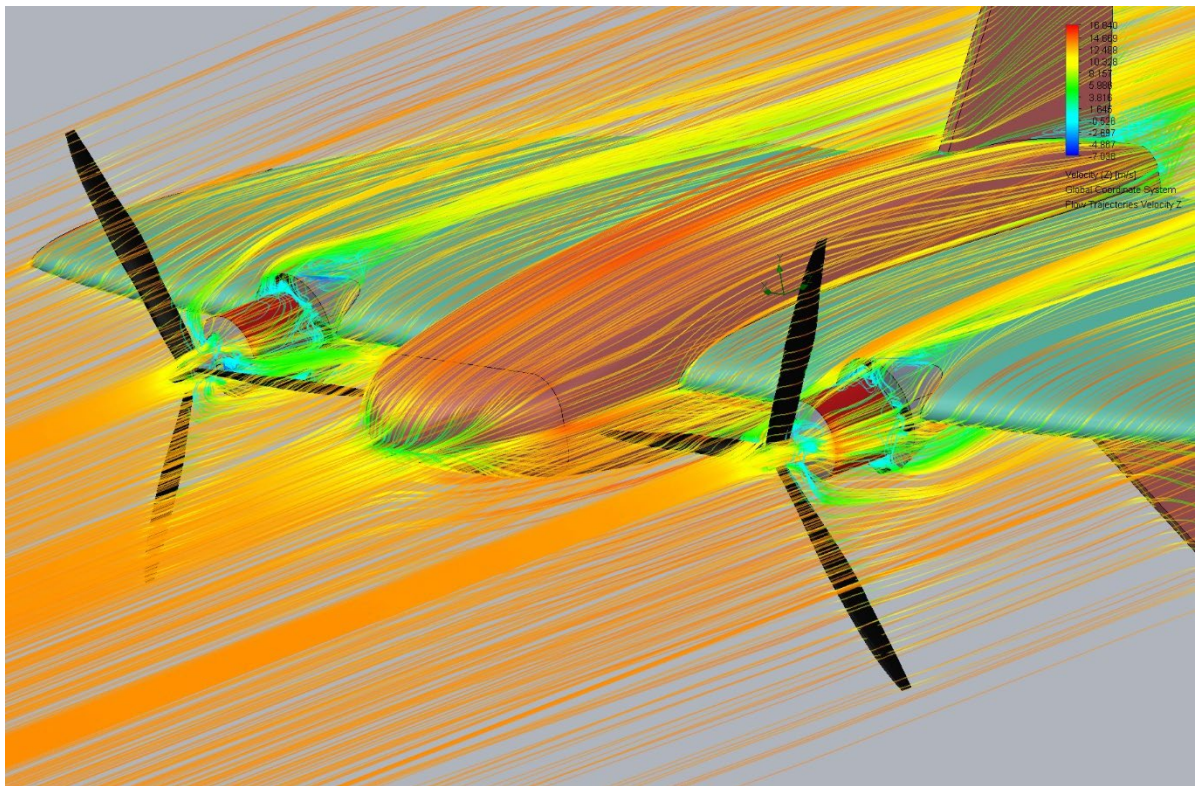


Figure 3.4 Isometric view of velocity (z) trajectories

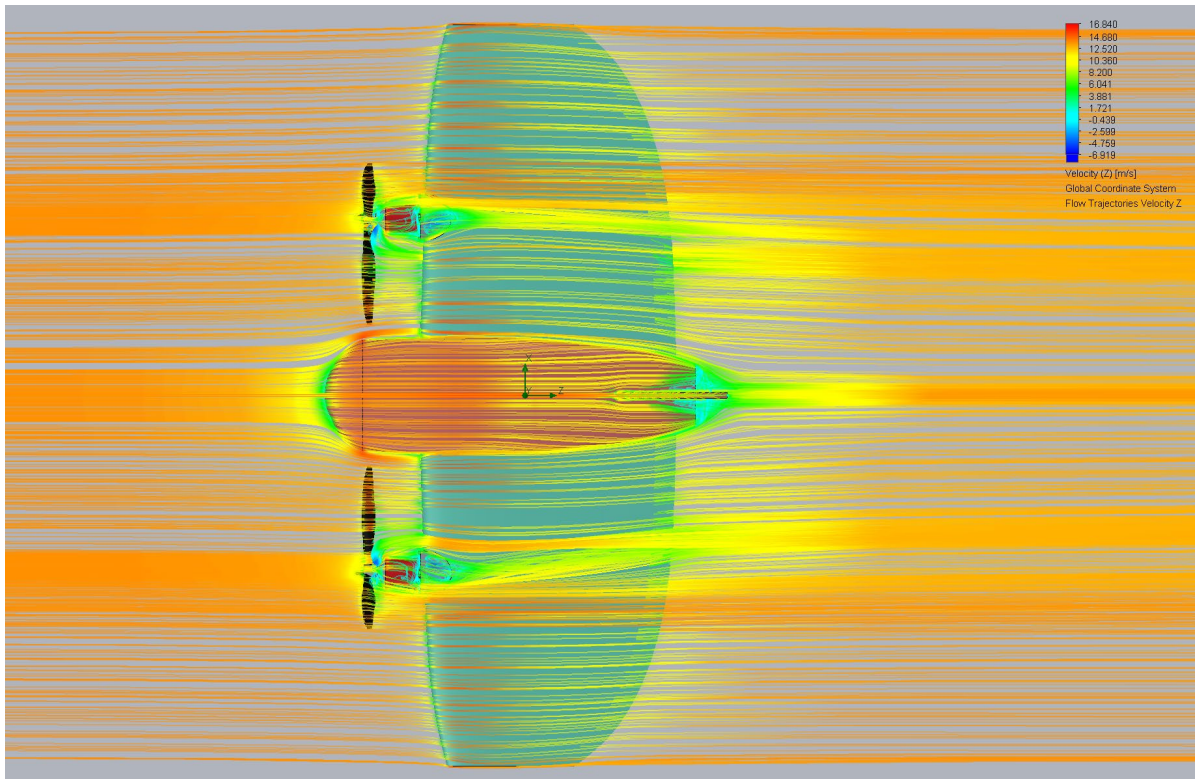


Figure 3.5 Top view of velocity (z) trajectories

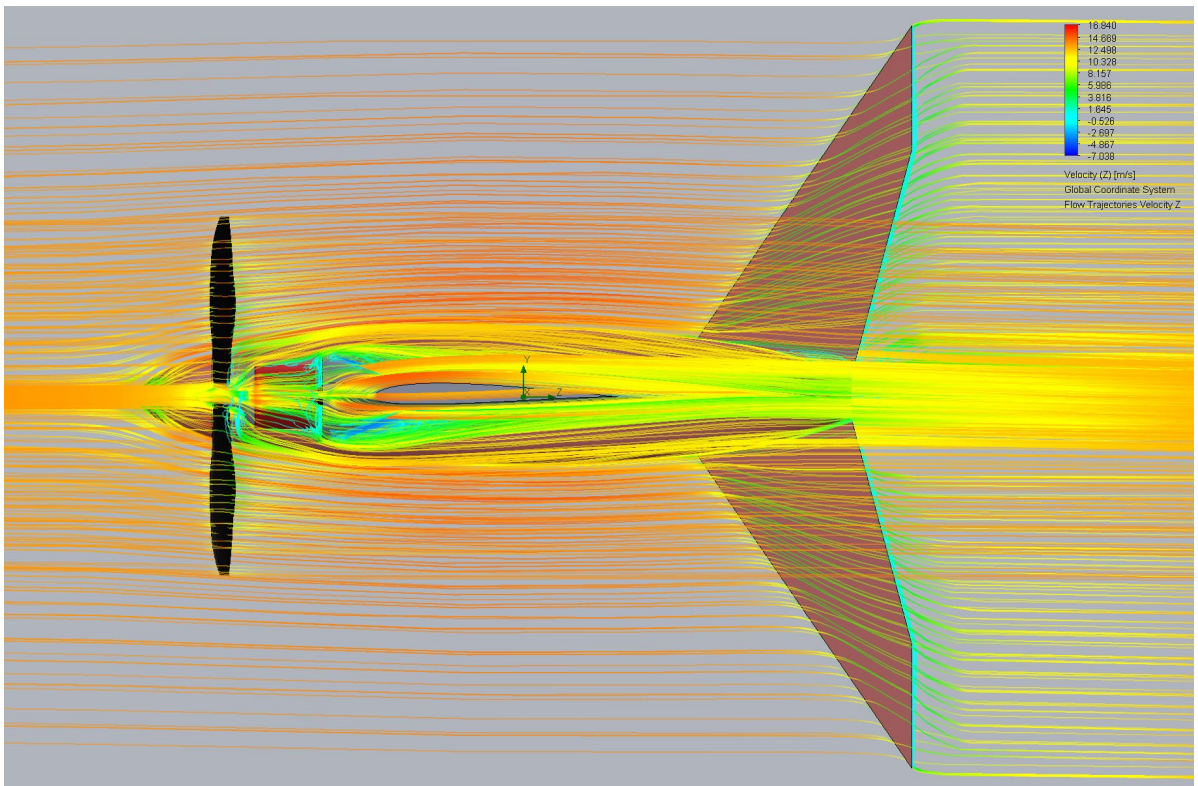


Figure 3.6 Right view of velocity (z) trajectories

When we look at the pressure distributions below, it is seen that the pressure increases in the nose of the aircraft and in the front parts of the wings.

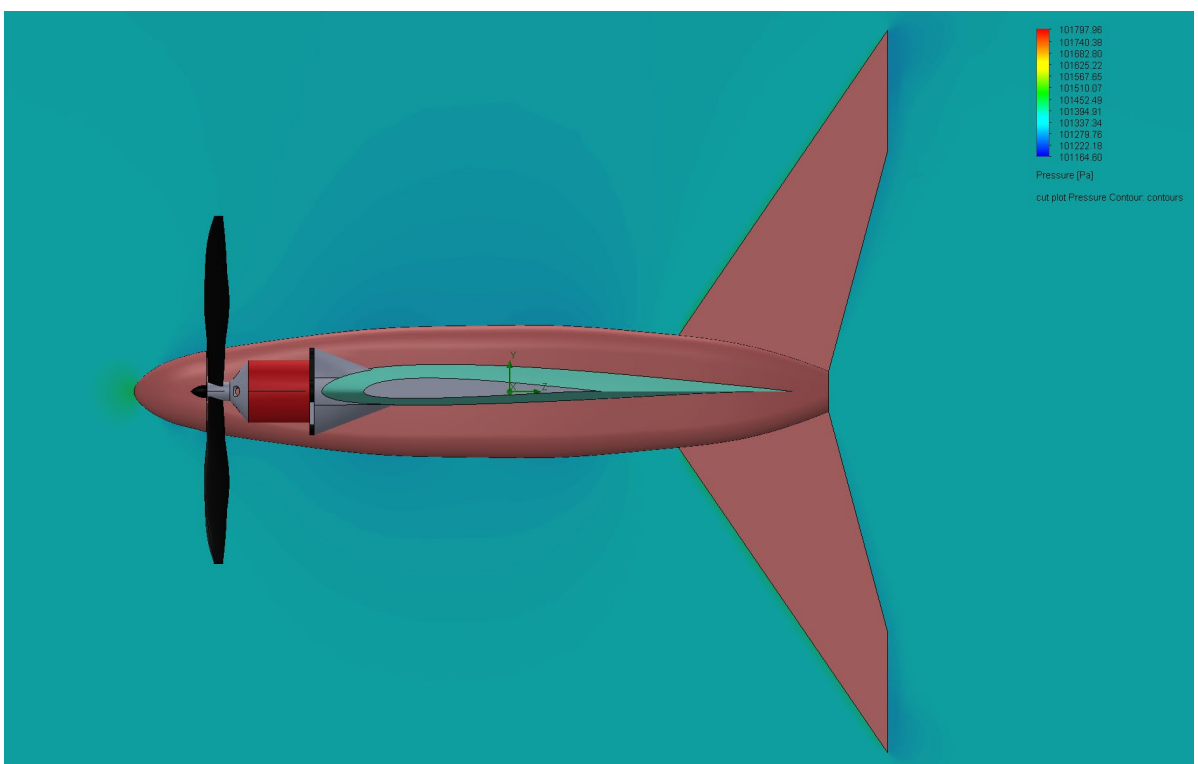


Figure 3.7 Right view of pressure contours

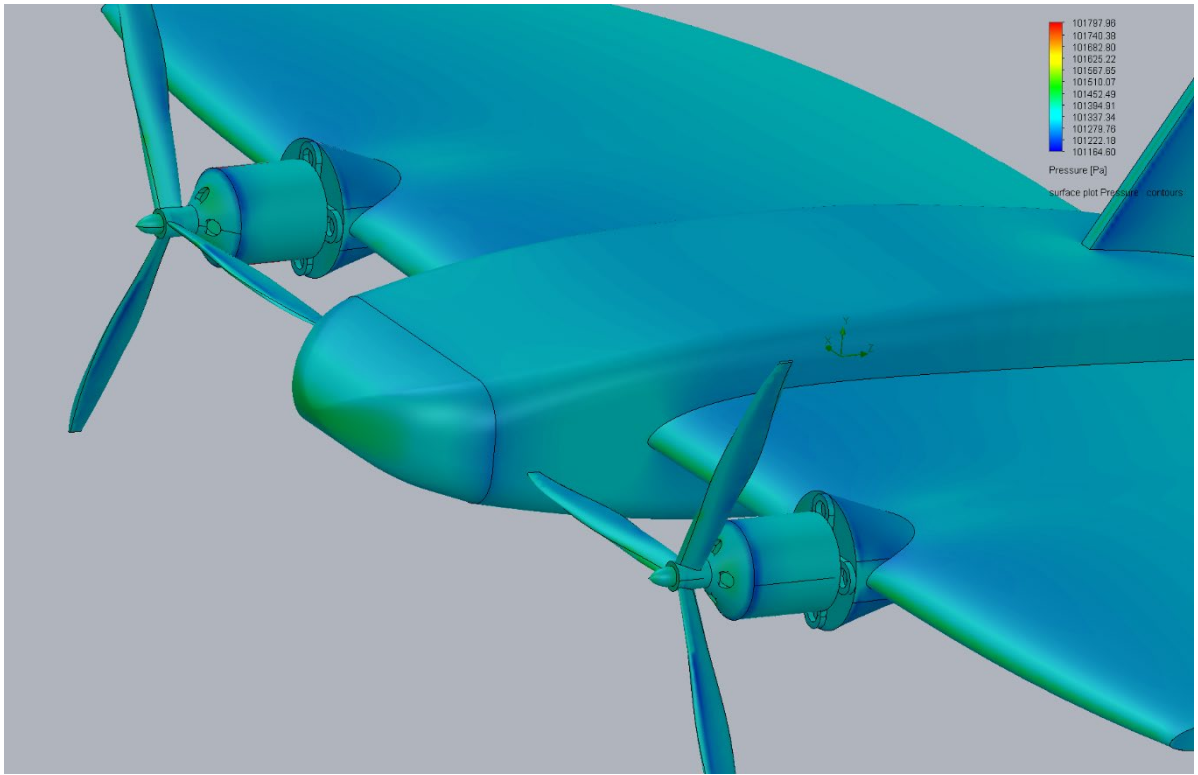


Figure 3.8 Isometric view of pressure contours

When we look at the temperature values of the gas on the body, it is seen that the temperature increases slightly in the front parts of the nose and the back part of the tail. In the upper and lower parts of the body, the temperature decreases slightly.

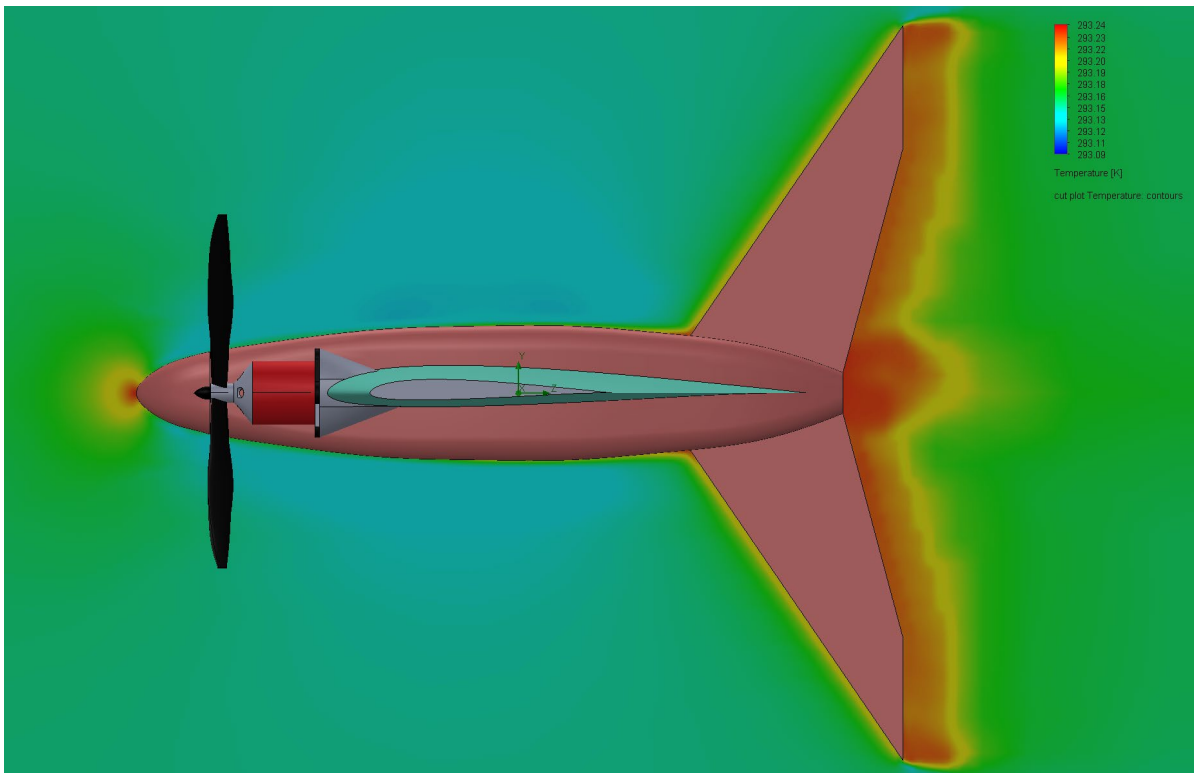


Figure 3.9 Right view of temperature contours

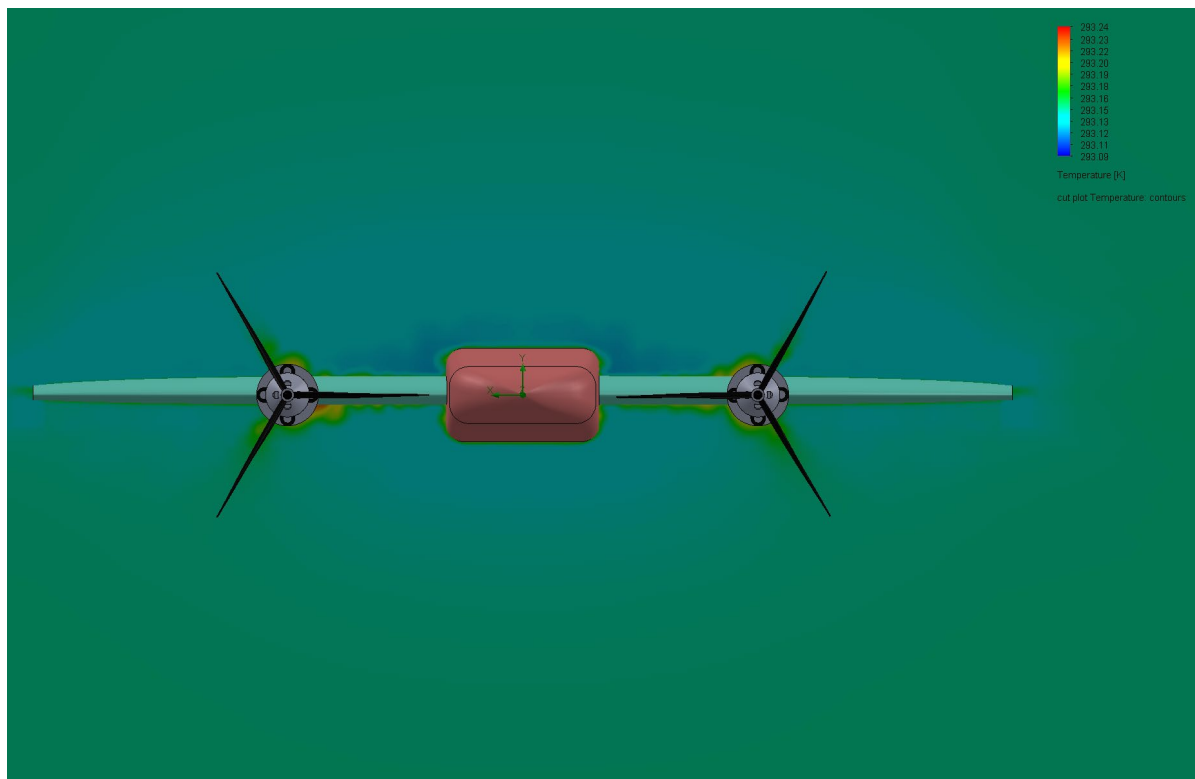


Figure 3.10 Front view of temperature contours

4. CONCLUSIONS

As a result, hybrid systems flying in tailsitter mode are becoming increasingly common and important. In this study, a suitable design was decided and designed. Then analyzed aerodynamically. After the design, the Reynolds number was determined as 300000. The speed of the drone was decided by using kinematic viscosity and characteristic length values. It is 13.54 m/s. Then, the lift/drag coefficient values were found by using the fluid velocity, reference wing area, air density and lift/drag force values from analysis.

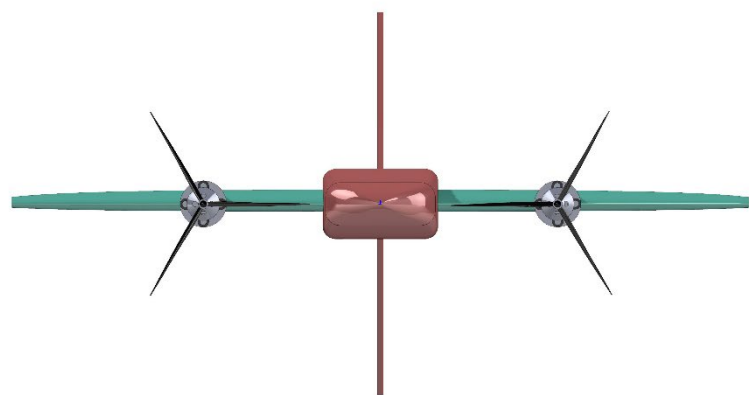
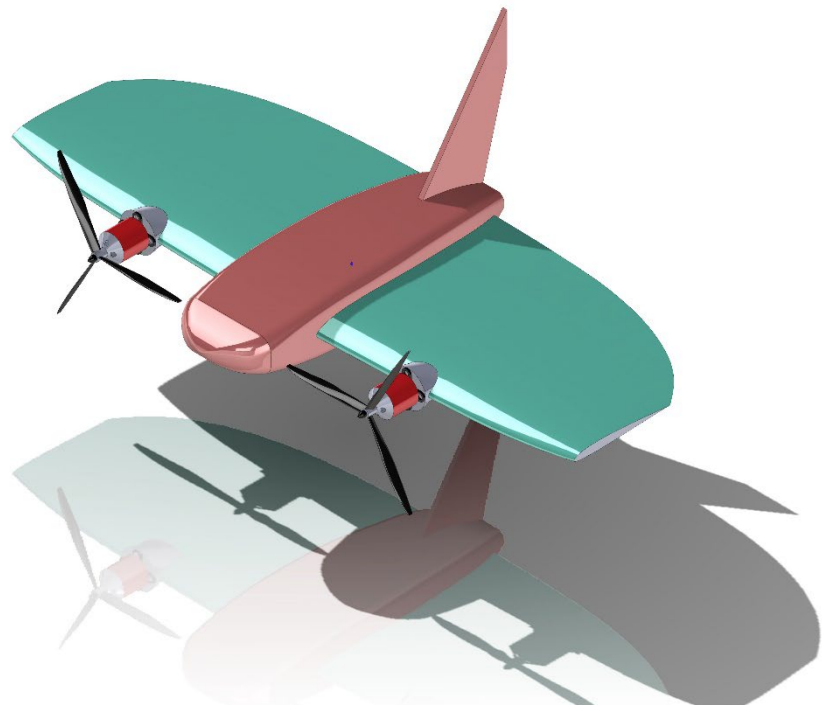
The lift coefficient value obtained was compared with the experimental findings and it was seen that a high accuracy rate was achieved. From the flow simulations performed on the aircraft, how the flow velocity, pressure and temperature are distributed and where they are concentrated are visually presented and analyzed. It is aimed to provide a roadmap for structural material selection and aerodynamic optimizations.

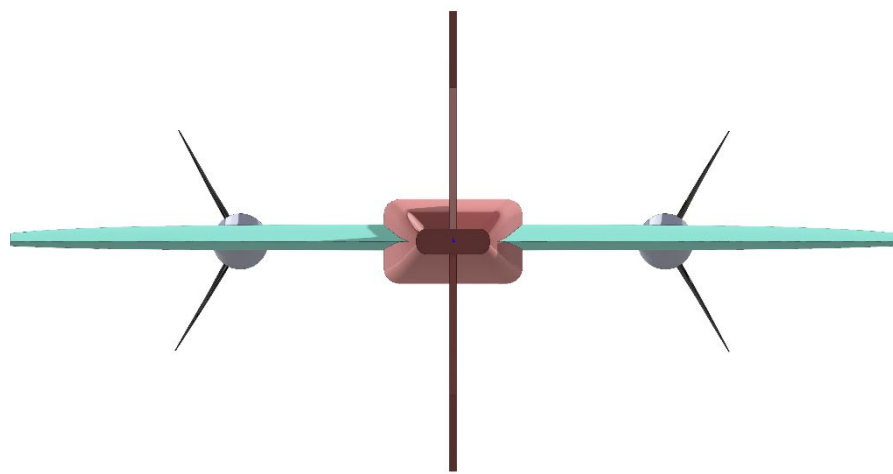
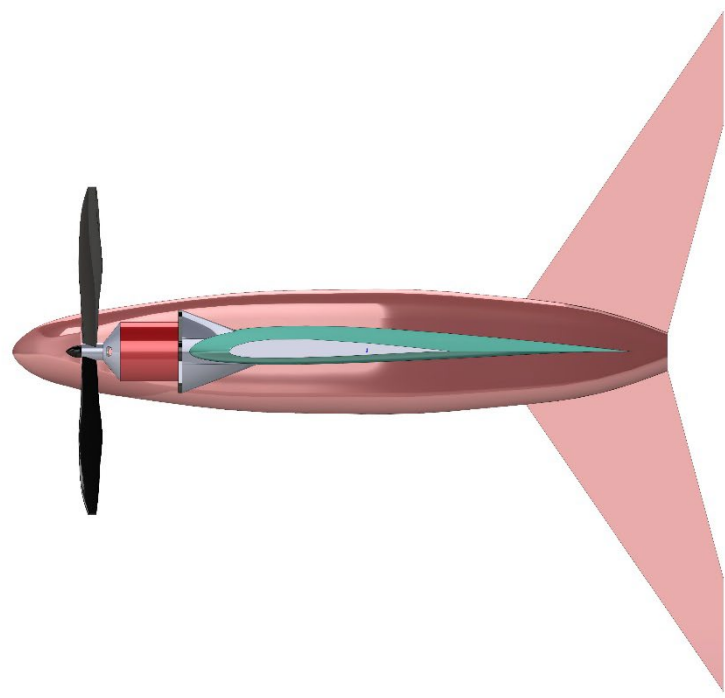
5. REFERENCES

- [1] Reynolds Number Calculator, <https://aerotoolbox.com/reynolds-number-calculator/>
- [2] Viscosity of Air, Dynamic and Kinematic, https://www.engineersedge.com/physics/viscosity_of_air_dynamic_and_kinematic_14483.htm
- [3] C.G. Calculator, https://www.scaleaero.com/CG_Calculator.htm
- [4] Density of air, https://en.wikipedia.org/wiki/Density_of_air
- [5] S. Selig, M., (1995). Summary of Low-Speed Airfoil Data, Department of Aeronautical and Astronautical Engineering University of Illinois at Urbana-Champaign, 1, 209.
- [6] Verling, S. (2017) Model-based Transition Optimization for a VTOL Tailsitter, 2017 IEEE International Conference on Robotics and Automation (ICRA), Singapore.
- [7] Chord (aeronautics), https://en.wikipedia.org/wiki/Chord_%28aeronautics%29

6. APPENDICES

More drawings of the Tailsitter drone from different perspectives:





More simulations and visual presentations on pressure distributions and flow trajectories:

